IEEE Photonics Journal
An IEEE Photonics Society Publication

Open Access

# Distributed Feedbacks for Time-Delay Signature Suppression of Chaos Generated From a Semiconductor Laser

Volume 4, Number 5, October 2012

**Song-Sui Li**
**Qing Liu**
**Sze-Chun Chan**

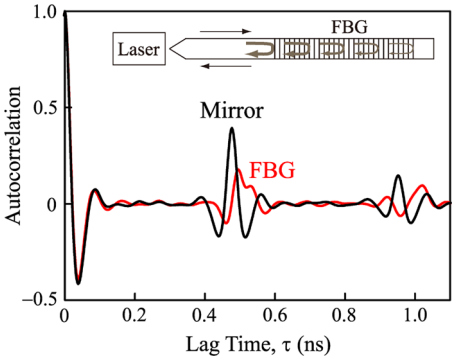


DOI: 10.1109/JPHOT.2012.2220759
1943-0655/$31.00 ©2012 IEEE

IEEE photonics SOCIETY

IEEE

# Distributed Feedbacks for Time-Delay Signature Suppression of Chaos Generated From a Semiconductor Laser

**Song-Sui Li,[1] Qing Liu,[1] and Sze-Chun Chan[1,2]**

[1]Department of Electronic Engineering, City University of Hong Kong, Kowloon, Hong Kong
[2]State Key Laboratory of Millimeter Waves, City University of Hong Kong, Kowloon, Hong Kong

*DOI: 10.1109/JPHOT.2012.2220759*
*1943-0655/$31.00 ©2012 IEEE*

Manuscript received September 2, 2012; revised September 20, 2012; accepted September 20, 2012. Date of current version October 3, 2012. This work was supported by the Research Grants Council of Hong Kong, China, under Project No. CityU 111210. Corresponding author: S. C. Chan (e-mail: scchan@cityu.edu.hk).

**Abstract:** Chaotic dynamics of a semiconductor laser subject to distributed feedbacks from a fiber Bragg grating (FBG) are investigated through detailed simulations. Because of distributed reflections along the FBG, the approach of FBG feedback performs better than the conventional approach of mirror feedback in concealing the feedback delay time in chaos generation. The time-delay signature obtained from the autocorrelation function decreases as the FBG bandwidth decreases, which is attributed to the associated increase in the FBG dispersion. Such time-delay signature suppression is generally observed over a range of feedback parameters. The dynamical mappings of the laser subject to FBG feedback reveal large regions of chaotic states, except when the FBG bandwidth is much narrower than the relaxation resonance frequency of the laser.

**Index Terms:** Semiconductor lasers, instabilities and chaos, fiber Bragg gratings.

## 1. Introduction

Nonlinear dynamics of semiconductor lasers under optical feedback have received revived attention for recent applications [1], [2]. The chaotic dynamics are particularly interesting because of their random-like broadband intensity waveforms, which inspired a number of emerging applications, including high-speed random bit generation, secure communication, and chaotic ranging [2]–[4]. In order to perturb a single-mode semiconductor laser into chaos, optical feedback from a properly adjusted mirror is often adopted. However, as for most time-delay systems, the output waveforms from the laser under mirror feedback often inherent pronounced autocorrelation near the feedback delay time, which is regarded as an undesirable time-delay signature [5]–[12]. The presence of the time-delay signature inevitably poses challenges for various applications. For instance, the sampling rate has to be carefully chosen in random bit generation, and ambiguities have to be resolved in chaotic ranging.

In this regard, detailed numerical simulations by Rontani *et al.* investigated the minimization of the time-delay signature through optimizing the feedback strength from the mirror [5]. Time-delay signature suppression was clearly achieved, but the suppression required a feedback delay time that was close to the inverse of the relaxation resonance frequency of the laser. Recently, some clever modifications on the mirror configurations for time-delay signature suppression have been proposed by Wu *et al.* [6]–[8]. Double feedback was adopted to completely suppress the time-delay signature. However, the suppression was achieved at the cost of increasing the setup complexity

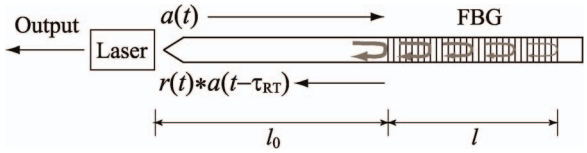


Fig. 1. Schematic of a semiconductor laser subject to distributed feedbacks from an FBG.

and demanding careful adjustments of the two feedback paths to ensure destructive superposition of the corresponding autocorrelation functions.

In this paper, we investigate time-delay signature suppression by employing a fiber Bragg grating (FBG) for feedback into the semiconductor laser. Different from the conventional use of a mirror for localized feedback, the proposed approach uses an FBG to provide distributed feedbacks along its length. The autocorrelation function around the feedback delay time is thereby broadened and suppressed accordingly. As a result, the time-delay signature is even smaller than the minimum value attainable using a mirror for the same feedback delay time. Moreover, the time-delay signature is found to decrease as the FBG bandwidth decreases, which is attributed to the associated increase in the dispersion of the FBG. Furthermore, chaos generation with time-delay signature suppression is generally observed over a range of feedback delay times, allowing flexibility in applications. The proposed approach of FBG feedback is easy to package, performs better than the conventional mirror feedback in time-delay signature suppression, and is much simpler to implement than the fine-tuned double feedback [6]. Feedbacks from Bragg gratings into semiconductor lasers have been investigated for applications such as wavelength tuning, noise reduction, frequency dynamics, and chaos control [13]–[15], although their chaotic dynamics for time-signature suppression remain to be examined.

## 2. Model

Fig. 1 shows the schematic of a single-mode semiconductor laser subject to distributed feedbacks from an FBG written on a single-mode fiber. The laser is described by the normalized charge carrier density $\tilde{n}(t)$ and the normalized intracavity optical field amplitude $a(t)$ in referencing to the free-running optical frequency. The laser emission to the left is the output. The emission to the right is directly coupled into the fiber so that a field amplitude proportional to $a(t)$ propagates toward the FBG. The field travels over a distance $l_0$ before it impinges on the input of the FBG, gets reflected by the FBG, and travels back to the laser. Denoting the impulse response of the FBG reflection by $r(t)$, the field amplitude coupling back to the laser is proportional to a convolution, i.e., $r(t) * a(t - \tau_{RT})$, where $\tau_{RT} = 2n_g l_0/c$ is the round-trip feedback delay time between the laser and the input of the FBG, $n_g = 1.45$ is the group index of the fiber, and $c$ is the speed of light in vacuum.

The rate equations that govern the laser dynamics are [16]–[18]

$$\frac{da}{dt} = \frac{1 - ib}{2}\left[\frac{\gamma_c\gamma_n}{\gamma_s\tilde{J}}\tilde{n} - \gamma_p\left(|a|^2 - 1\right)\right] + \gamma_c\xi_f e^{i\theta} r(t) * a(t - \tau_{RT}) \tag{1}$$

$$\frac{d\tilde{n}}{dt} = -\left(\gamma_s + \gamma_n|a|^2\right)\tilde{n} - \gamma_s\tilde{J}\left(1 - \frac{\gamma_p}{\gamma_c}|a|^2\right)\left(|a|^2 - 1\right) \tag{2}$$

where $\gamma_c = 5.36 \times 10^{11}$ s$^{-1}$ is the cavity decay rate, $\gamma_s = 5.96 \times 10^9$ s$^{-1}$ is the spontaneous carrier relaxation rate, $\gamma_n = 7.53 \times 10^9$ s$^{-1}$ is the differential carrier relaxation rate, $\gamma_p = 1.91 \times 10^{10}$ s$^{-1}$ is the nonlinear carrier relaxation rate, $\tilde{J} = 1.222$ is the normalized bias current above threshold, $b = 3.2$ is the linewidth enhancement factor, $\theta = 0$ is the feedback phase, and $\xi_f$ is the normalized feedback strength proportional to the coupling efficiency between the laser and the fiber. The laser parameters correspond to a relaxation resonance frequency of $f_r = 10.25$ GHz and were extracted from a commercial communication laser [18].

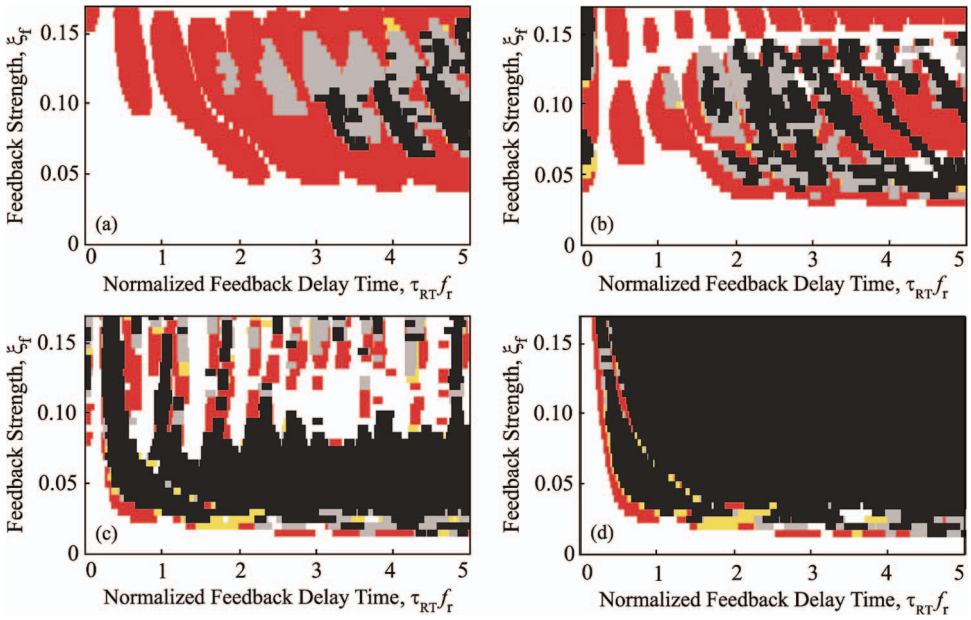


Fig. 2. Mappings of the dynamical states when $\Delta f/f_r$ is (a) 0.32, (b) 0.65, (c) 3.2, and (d) 13. Regions of stable states (white), period-one states (red), quasi-periodic states (gray), period-doubled states (yellow), and chaotic states (black) are identified.

The FBG has a uniform coupling coefficient $\kappa$ along its length $l$ such that the frequency response of the reflection is [19], [20]

$$r(\Omega) = \kappa^* \left[ \delta - \mathrm{i}\sqrt{|\kappa|^2 - \delta^2}\coth\sqrt{|\kappa|^2 - \delta^2}l \right]^{-1} \tag{3}$$

where $\delta = -n_g\Omega/c$ quantifies the phase mismatch between the counterpropagating modes with angular frequency detuning $\Omega$ away from the Bragg resonance. The response in (3) is obtained from the coupled-mode theory instead of the simplified Lorentzian model [19], [21]. Assuming zero detuning between the free-running laser and the FBG, the impulse response $r(t)$ is simply the inverse Fourier transform of $r(\Omega)$. The results presented in the rest of this paper focus on real $\kappa$ with $\Delta f = c\kappa/\pi n_g$ being a good approximation of the full-width at half-maximum FBG bandwidth when the FBG is highly reflective. Numerical simulations are conducted based on second-order Runge–Kutta integration of (1)–(3) with time step 2.38 ps for a time span of 1.25 $\mu$s. The FBG is specified by $(\Delta f, l)$, whereas the feedback into the laser is specified by $(\xi_f, \tau_{RT})$.

It is worth mentioning that the rate-equation model in (1)–(2) is a generic model for arbitrary feedback impulse response $r(t)$, which is causal for any physical reflections. The optical gain of the laser is linearized in the modeling as proposed and experimentally verified in previous works [17]. For FBG feedback, the impulse response $r(t)$ is evaluated from an inverse Fourier transform of $r(\Omega)$ in (3). The laser at time $t$ is affected by its emission at and before $t - \tau_{RT}$. For mirror feedback, the impulse response $r(t)$ can be set as $\delta(t)$, where the rate equations in (1)–(2) simply reduce to the conventional Lang–Kobayashi model [16]. The laser at time $t$ is affected by its emission at exactly $t - \tau_{RT}$ only.

## 3. Dynamical Mappings

Fig. 2 shows the mappings of the dynamical states of the laser in the feedback parameter space $(\xi_f, \tau_{RT})$. Maps with different FBG bandwidths $\Delta f$ are shown in Fig. 2(a)–(d), where the FBG length $l$ is kept constant at 20 mm. The stable states, period-one states, quasi-periodic states, period-doubled states, and chaotic states are identified according to the time series of the output intensity obtained from the simulations [22]. In Fig. 2(a) with $\Delta f/f_r = 0.32$, the laser remains stable over a

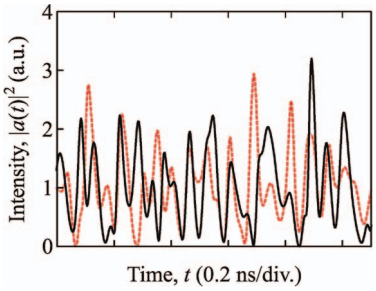


Fig. 3. Chaotic output intensity when $(\xi_f, \tau_{RT}) = (0.078, 0.47\ \text{ns})$. The laser is subject to mirror feedback (black) or FBG feedback (red).

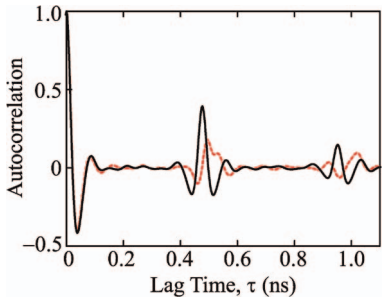


Fig. 4. Autocorrelation function of the chaotic output intensity when $(\xi_f, \tau_{RT}) = (0.078, 0.47\ \text{ns})$. The laser is subject to mirror feedback (black) or FBG feedback (red).

large region on the map. This is because the FBG is too narrow to strongly feedback any optical sidebands generated by the relaxation oscillations of the laser at $f_r$. The relaxation oscillations thus remain damped for small $\xi_f$ [18]. The relaxation oscillations can nonetheless be undamped with sufficiently large $\xi_f$, which results in isolated regions of period-one oscillation states on the map. Interestingly, period-one oscillation states are found even when $\tau_{RT} = 0$ for $\xi_f > 0.15$ because the feedback light still experiences some delay during distributed reflections in the FBG. Regions of quasi-periodic states and chaotic states are also found on the map. Therefore, even though the chaos regions are relatively small in Fig. 2(a), quasi-periodic routes to chaos are identified, as for most semiconductor lasers subject to feedbacks [3], [22], [23]. In Fig. 2(b) with $\Delta f/f_r = 0.65$, the FBG bandwidth is increased, and more chaos regions are found on the map. In Fig. 2(c) with $\Delta f/f_r = 3.2$, the FBG bandwidth is further increased such that the chaos regions are much enlarged and merge together, which adds flexibility to the choice of $\tau_{RT}$ in chaos generation. In Fig. 2(d) with $\Delta f/f_r = 13$, the map is mainly occupied by the chaotic states. Because $\Delta f$ is much larger than $f_r$ and the bandwidths of semiconductor laser dynamics are typically limited by $f_r$ [24], the FBG behaves essentially as a mirror with no frequency selectivity. The map is nearly identical to one obtained from conventional mirror feedback [3]. Overall, Fig. 2 shows that chaos regions can be identified for the laser subject to FBG feedback, although the chaos regions shrink as the FBG bandwidth decreases.

## 4. Time-Delay Signature

Chaotic states generated by FBG feedback and mirror feedback are compared in Figs. 3 and 4. The results of FBG feedback with $\Delta f/f_r = 2.8$ and $l = 20$ mm are shown in red. The results of mirror feedback obtained by setting $r(t) = \delta(t)$ in (1) are shown in black. The feedback parameters are fixed at $(\xi_f, \tau_{RT}) = (0.078, 0.47\ \text{ns})$ for both cases. The time series of the normalized intensity $|a(t)|^2$ are shown in Fig. 3, where the associated autocorrelation functions of $|a(t)|^2$ are plotted against the lag time $\tau$ in Fig. 4. As the black curve in Fig. 4 shows, the feedback delay time $\tau_{RT}$ clearly manifests

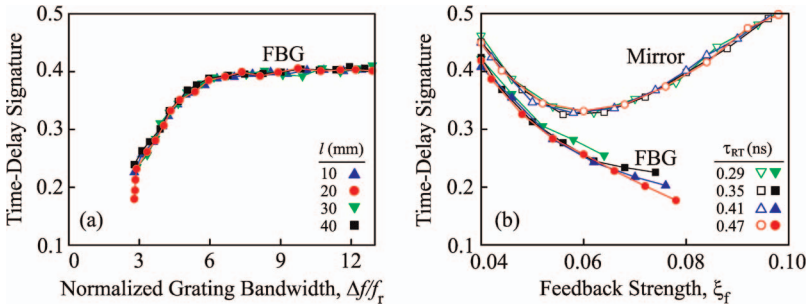


Fig. 5. Time-delay signature (a) as a function of $\Delta f/f_r$ at different $l$ and (b) as a function of $\xi_f$ at different $\tau_{RT}$ using FBG feedback or mirror feedback.

itself as a strong autocorrelation peak at $\tau = \tau_{RT}$ when the laser is under mirror feedback. The time-delay signature, which is defined as the maximum magnitude of autocorrelation for $\tau$ between $\tau_{RT} \pm (1/2)f_r^{-1}$ [6], is as high as 0.4. However, by replacing the mirror with the FBG, the red curve in Fig. 4 exhibits broadening and suppression of the autocorrelation peak, where the time-delay signature decreases by as much as 55%.

Time-delay signature suppression is achieved because of the distributed reflections in FBG feedback instead of the localized reflection in mirror feedback. The suppression can also be related to the chromatic dispersion of the FBG reflection, where the group delay is different for different optical frequency components of the chaotic emission. Fig. 5(a) illustrates the dependence of the time-delay signature on the FBG bandwidth $\Delta f$ and length $l$. The feedback parameters are maintained at $(\xi_f, \tau_{RT}) = (0.078, 0.47\ \text{ns})$, which correspond to a point inside the chaos regions in Fig. 2(c)–(d). At this point, the laser continually remains in chaos when $\Delta f/f_r$ is tuned from infinity down to 2.8. However, further decrease in $\Delta f/f_r$ can drive the laser into other states.

The group delay associated with the FBG reflection can be approximated by $(\pi\Delta f)^{-1}[1+(1/2)(\Omega/\pi\Delta f)^2]$, where the term with $\Omega$ signifies the dispersion of the group delay [20]. When $\Delta f$ decreases, the dispersion increases, which causes the autocorrelation peak to broaden. The time-delay signature reduces accordingly in Fig. 5(a). When $l$ is changed, the dispersion remains unchanged, and thus, the time-delay signature also remains unchanged in Fig. 5(a).

Furthermore, Fig. 5(b) examines the time-delay signature of the chaotic states as a function of the feedback strength $\xi_f$, where the delay time $\tau_{RT}$ is varied from 0.29 to 0.47 ns. The open symbols are obtained using mirror feedback. The closed symbols are obtained using FBG feedback with $\Delta f/f_r = 2.8$ and $l = 20$ mm. As $\xi_f$ increases, the time-delay signature from mirror feedback reaches a minimum at approximately $\xi_f = 0.06$, but the signature from FBG feedback decreases monotonically. The time-delay signature is always decreased when mirror feedback is replaced by FBG feedback under the same $(\xi_f, \tau_{RT})$. Hence, Fig. 5 shows that FBG feedback is a convenient approach to generating chaos with a suppressed time-delay signature for different $\tau_{RT}$, where the signature subsides as the FBG bandwidth decreases and is independent of the FBG length.

## 5. Conclusion

In summary, chaos generation in a semiconductor laser under FBG feedback is investigated. FBG feedback outperforms conventional mirror feedback in the suppression of the time-delay signature. The time-delay signature suppression is attributed to the distributed reflections in the FBG or, equivalently, the dispersion of the reflection group delay. Therefore, the suppression improves as the FBG bandwidth decreases and is independent of the length of the FBG. Additionally, mappings of different dynamical states in the feedback parameter space $(\xi_f, \tau_{RT})$ reveal large regions of chaotic states, except when the FBG bandwidth $\Delta f$ is much narrower than the relaxation resonance frequency $f_r$ of the laser. The time-delay signature is generally suppressed by the FBG feedback independent of the feedback parameters. Improvements on the signature suppression through optimizing the grating designs can be further explored.

## References


[1] S. Donati, "Developing self-mixing interferometry for instrumentation and measurements," *Laser Photon. Rev.*, vol. 6, no. 3, pp. 393–417, May 2012.

[2] A. Uchida, K. Amano, M. Inoue, K. Hirano, S. Naito, H. Someya, I. Oowada, T. Kurashige, M. Shiki, S. Yoshimori, K. Yoshimura, and P. Davis, "Fast physical random bit generation with chaotic semiconductor lasers," *Nat. Photon.*, vol. 2, no. 12, pp. 728–732, Dec. 2008.

[3] L. E. Larson, J. M. Liu, and L. S. Tsimring, *Digital Communications Using Chaos and Nonlinear Dynamics*. New York: Springer-Verlag, 2006.

[4] W. T. Wu, Y. H. Liao, and F. Y. Lin, "Noise suppressions in synchronized chaos lidars," *Opt. Exp.*, vol. 18, no. 25, pp. 26155–26162, Dec. 2010.

[5] D. Rontani, A. Locquet, M. Sciamanna, and D. S. Citrin, "Loss of time-delay signature in the chaotic output of a semiconductor laser with optical feedback," *Opt. Lett.*, vol. 32, no. 20, pp. 2960–2962, Oct. 2007.

[6] J. G. Wu, G. Q. Xia, and Z. M. Wu, "Suppression of time delay signatures of chaotic output in a semiconductor laser with double optical feedback," *Opt. Exp.*, vol. 17, no. 22, pp. 20124–20133, Oct. 2009.

[7] J. G. Wu, G. Q. Xia, X. Tang, X. D. Lin, T. Deng, L. Fan, and Z. M. Wu, "Time delay signature concealment of optical feedback induced chaos in an external cavity semiconductor laser," *Opt. Exp.*, vol. 18, no. 7, pp. 6661–6666, Mar. 2010.

[8] J. G. Wu, Z. M. Wu, G. Q. Xia, and G. Y. Feng, "Evolution of time delay signature of chaos generated in a mutually delay-coupled semiconductor lasers system," *Opt. Exp.*, vol. 20, no. 2, pp. 1741–1753, Jan. 2012.

[9] M. W. Lee, P. Rees, K. A. Shore, S. Ortin, L. Pesquera, and A. Valle, "Dynamical characterisation of laser diode subject to double optical feedback for chaotic optical communications," *IEE Proc.-Optoelectron.*, vol. 152, no. 2, pp. 97–102, Apr. 2005.

[10] A. Prasad, Y. C. Lai, A. Gavrielides, and V. Kovanis, "Complicated basins in external-cavity semiconductor lasers," *Phys. Lett. A*, vol. 314, no. 1/2, pp. 44–50, Jul. 2003.

[11] G. Van der Sande, M. C. Soriano, I. Fischer, and C. R. Mirasso, "Dynamics, correlation scaling, and synchronization behavior in rings of delay-coupled oscillators," *Phys. Rev. E, Stat. Phys. Plasmas Fluids Relat. Interdiscip. Top.*, vol. 77, no. 5, pp. 055202-1–055202-4, May 2008.

[12] M. A. Arteaga, M. Valencia, M. Sciamanna, H. Thienpont, M. Lopez-Amo, and K. Panajotov, "Experimental evidence of coherence resonance in a time-delayed bistable system," *Phys. Rev. Lett.*, vol. 99, no. 2, pp. 023903-1–023903-4, Jul. 2007.

[13] S. Furst, S. Yu, and M. Sorel, "Fast and digitally wavelength-tunable semiconductor ring laser using a monolithically integrated distributed Bragg reflector," *IEEE Photon. Technol. Lett.*, vol. 20, no. 23, pp. 1926–1928, Dec. 2008.

[14] M. Yousefi and D. Lenstra, "Dynamical behavior of a semiconductor laser with filtered external optical feedback," *IEEE J. Quantum Electron.*, vol. 35, no. 6, pp. 970–976, Jun. 1999.

[15] I. V. Ermakov, V. Z. Tronciu, P. Colet, and C. R. Mirasso, "Controlling the unstable emission of a semiconductor laser subject to conventional optical feedback with a filtered feedback branch," *Opt. Exp.*, vol. 17, no. 11, pp. 8749–8755, May 2009.

[16] R. Lang and K. Kobayashi, "External optical feedback effects on semiconductor injection laser properties," *IEEE J. Quantum Electron.*, vol. QE-16, no. 3, pp. 347–355, Mar. 1980.

[17] J. M. Liu and T. B. Simpson, "Four-wave mixing and optical modulation in a semiconductor laser," *IEEE J. Quantum Electron.*, vol. 30, no. 4, pp. 957–965, Apr. 1994.

[18] C. Cui and S. C. Chan, "Performance analysis on using period-one oscillation of optically injected semiconductor lasers for radio-over-fiber uplinks," *IEEE J. Quantum Electron.*, vol. 48, no. 4, pp. 490–499, Apr. 2012.

[19] T. Erdogan, "Fiber grating spectra," *J. Lightwave Technol.*, vol. 15, no. 8, pp. 1277–1294, Aug. 1997.

[20] S. Longhi, M. Marano, P. Laporta, O. Svelto, and M. Belmonte, "Propagation, manipulation, and control of picosecond optical pulses at 1.5 $\mu$m in fiber Bragg gratings," *J. Opt. Soc. Amer. B, Opt. Phys.*, vol. 19, no. 11, pp. 2742–2757, Nov. 2002.

[21] H. Erzgraber and B. Krauskopf, "Dynamics of a filtered-feedback laser: Influence of the filter width," *Opt. Lett.*, vol. 32, no. 16, pp. 2441–2443, Aug. 2007.

[22] F. Y. Lin and J. M. Liu, "Nonlinear dynamics of a semiconductor laser with delayed negative optoelectronic feedback," *IEEE J. Quantum Electron.*, vol. 39, no. 4, pp. 562–568, Apr. 2003.

[23] J. Ohtsubo, "Chaos synchronization and chaotic signal masking in semiconductor lasers with optical feedback," *IEEE J. Quantum Electron.*, vol. 38, no. 9, pp. 1141–1154, Sep. 2002.

[24] F. Y. Lin, Y. K. Chao, and T. C. Wu, "Effective bandwidths of broadband chaotic signals," *IEEE J. Quantum Electron.*, vol. 48, no. 8, pp. 1010–1014, Aug. 2012.